

High Energy Density Magnesium-Air Battery for Shipping, Rail and Aviation Electrification and Grid Storage

Kurt Lindenthal, Tyler Riggs, Jacqueline Simon Villacis, Edward Miller

Worcester Polytechnic Institute

Major Qualifying Project

Advisor: Professor Adam Powell

April 24th, 2023

Acknowledgments: Mahya Shahabi (Ph.D.), Michael Collins, Nicholas Masse, Heath Bastow,

Amanda Lota, Connor Cumming

This report represents the work of one or more WPI undergraduate students submitted to the faculty as evidence of completion of a degree requirement. WPI routinely publishes these reports on the web without editorial or peer review.

Table of Contents

Abstract	3
Introduction	4
Background	4
Methodology	9
Results	13
Conclusion	20
Works Cited	21
Appendix of Tables	23

Abstract

Magnesium is a very common and highly reactive metal that is primarily found in our oceans, and in metal scrap. Magnesium is commonly used to produce metal alloys, but its reactivity makes it useful for power generation. This project focuses on the development of a magnesium-air battery for use in grid storage and cargo ship propulsion. The magnesium-air battery has more energy density, but less power density, than typical lithium-ion batteries, so it can be used for long-term power. The project focuses on studying the corrosion of the battery cathode and surrounding insulation under standard operating conditions. These conditions included an operating temperature of 550 Celsius and molten salt as the electrolyte. Several types of materials were tested, and each material was studied under a microscope for physical damage and corrosion. The project also includes an FMEA analysis of the proposed pilot battery.

Introduction

This Major Qualifying Project the team worked with Professor Adam Powell and graduate students from the Energy Metals Research Group (EMRG). The project focuses on the Magnesium-Air Battery, which uses Mg^{2+} and O^{2-} ions from the magnesium anode and air cathode, respectively. These sources and subsequent half reactions have a theoretical open-circuit voltage of 2.6 V, and the ions solidify into MgO molecules. The battery operates at approximately 550 °C, which is its main detriment. However, magnesium has significantly higher energy density than lithium or other electrolytes, so electricity can be stored in these batteries in large, cheap quantities. The lab-scale prototype, still in the early stages of its development, hopes to offer an alternative solution to energy storage and large naval vessel power from the more mainstream lithium ion batteries.

The objectives of this project were as follows. First, the battery requires an insulation material, most likely some type of firebrick. However, the battery conditions accelerate corrosion of internal parts, so any internal insulation would need to withstand these highly corrosive conditions. As such, the first objective of the project was to test two different types of firebrick, refractory and high-alumina, and see which type was more suitable for the battery conditions.

The second objective of the project was to study the effect of the battery on different cathode mesh materials. The cathode mesh is necessary to prevent salt from flowing into the cathode, while allowing air through. The two materials under study were porous nickel and porous titanium mesh. Both mesh types were used in battery experiments, and studied afterwards for signs of corrosive damage.

The final objective was to study the safety risks and protocols of the proposed battery through FMEA analysis. Since the battery has only progressed to a pilot cell and containment systems, the safety issues if the battery was brought to scale have not been examined. As such, it is necessary to study the different risks, and develop protocols to counteract these risks. These objectives are meant to assist the development of the battery, and eventually lead to an upscaled cell for industrial use.

Background

The Magnesium-Air battery is a prototype battery with higher energy storage levels than lithium ion batteries. Magnesium air batteries present an eco-friendly alternative compared to other battery options while at a lower production cost. With greater availability of magnesium than lithium through desalination, it is a more practical and energy-efficient option. One potential market of the magnesium air battery is to power long distance travel such as, shipping, rail, and aviation. Another potential market for the battery design is to act as electrical grid storage for renewable energy storage, such as wind and solar power. Magnesium batteries potentially have a significantly higher energy density than lithium batteries, which would allow for long term storage of electricity, which is often cheaper per kilowatt hour than fossil fuels. In addition, the energy density of magnesium is suitable for long distance transport, such as aircraft, rail, and

especially cargo ships. Cargo ships in particular use low grade bunker fuel, which is a high pollution, low efficiency fuel. A suitable battery design would not only be more environmentally suitable, but could also exceed the engine efficiency of bunker fuel, allowing for a cheaper fuel source for cargo shipping, which accounts for most international shipping methods.

The proposed battery design evidently requires large amounts of magnesium metal to produce the electrodes in the battery. Luckily, the second most common cation in seawater, behind sodium, is magnesium. This means that desalinization is a particularly effective way to recover large amounts of magnesium, especially with regard to the brine byproducts of said process. Seawater contains approximately 1250 tons of magnesium per cubic kilometer, meaning that it is a very viable resource for new magnesium metal. In fact, as of 1990, more than 33% of the world's magnesium compound production was from seawater, and this large production share continues to be the case today (1). Magnesium in seawater typically exists as $MgCl_2$, which is typically extracted through the following process. This extraction is performed by adding lime or caustic soda to seawater bitterns, thereby precipitating $Mg(OH)_2$. HCl can then be added to the precipitate, forming magnesium chloride (1). There are already established processes for performing extraction, the most common being electrolysis.

Magnesium recycling is also a very popular and profitable method of obtaining magnesium. Magnesium is commonly used as a component in a variety of metal alloys, so there are plenty of machining scraps. Die casting of metal alloys is an especially plentiful source of recycled magnesium, whether the metal is recycled internally or externally to the manufacturer. Automotive parts are one of the largest sources of magnesium scrap in particular, but many industries produce magnesium scrap as well (5). In terms of designing a magnesium-air battery, obtaining the necessary magnesium metal for mass production will not be particularly difficult, given the amount of stable sources there are.

The focus of our study will be on cathode materials/corrosion, battery insulation material/design, and battery safety. The challenge we will face will be coordinating with the existing team to come up with the best solutions that will integrate well with other aspects of the battery that our team is not as involved in. This MQP should provide the overall battery project with a more fundamental understanding and plans for these specific categories.

The cathode of the proposed battery design is under particularly unique conditions. Due to the presence of the molten salt and air in the battery, the cathode material will be subjected to conditions that typically accelerate corrosion. Therefore, the use of corrosion resistant materials is advised, and there are a few main options, which are as follows. The first possible option is porous nickel. Porous nickel, like most porous metals, is produced by sintering and processing metal powder. In general, porous metals tend to be strong and lightweight materials, and can withstand very high temperatures. Porous nickel is generally resistant to corrosion under normal atmospheric conditions, as well as alkaline conditions (2). However, the battery conditions are fairly unique, so there is very little research on how porous nickel would respond to these conditions. The second, and final possible option is porous titanium. Porous titanium is produced through metal powder processing, but is slightly different from nickel in several ways. Titanium

is generally corrosion resistant, especially under high heat conditions and in chloride environments (11). Since the battery operates at about 900 °C, and contains a chloride salt, porous titanium is a feasible option, and is worth testing. The final feasible material is stainless steel, preferably Kanthal. These materials have not been tested widely under the operating conditions of the battery, but it can be assumed that the molten salt will accelerate corrosion rates on the cathode material. Since these materials can already withstand corrosion to a good degree, it may be wise to test each material, and determine which one has the slowest corrosion rate. In general, the slowest possible corrosion rate will be the most ideal for the battery.

There are many benefits to the battery, but a major requirement for its adoption for commercial utilization will be its overall safety. With the battery possessing multiple failure points with varying levels of severity it is important all possible points are looked into and safety protocols and designs are put in place to either stop or lessen the damages caused. There are many safety hazards which must be considered before further application of a magnesium-air battery. This includes elements such as the following:

- Plating/ stripping cycles
- Short circuits
- Fire hazards
- Thermal runaway
- Charging regulations
- Proper ventilation
- High operating temperatures
- Parasitic reactions

The magnesium-air battery is a considerably more cost-efficient alternative to the lithium-ion battery. With a magnesium base, the formation of dendrites can potentially be prevented. This could result in issues with the battery's anode over time, which is a common problem among lithium-ion batteries.

Another issue to consider are plating stripping cycles which can lead to degradation of a battery over time. Plating in a battery occurs when metal has been deposited on the surface of the anode of the battery during charging. In an intercalation anode, such as graphite in a lithium-ion battery, this is a problem, as lithium metal could react with other battery components; in this case plating of magnesium metal is the desired charging reaction. Stripping of a battery occurs when there is an electrochemical oxidation of the surface atoms on the battery which causes a release of cations onto the electrolyte during discharge. Cations as a positively charged ion become attracted to the cathode of the battery.

Another safety issue to take into account are short circuits which occur when metal depositing becomes uneven throughout the charging cycle of the battery leading to the formation of dendrites on the anode. To prevent the possibility of a short circuit it is important to take precautions such as using fuses. Fuses create a break in the circuit of the battery if there is unsafe current flow. Basic circuit breaker maintenance along with electrical inspections must also be performed to avoid a short circuitry in the system (4).

Thermal runaway occurs when there is an overproduction of energy over the battery's capacity. This can be avoided through proper storage temperature of the battery, proper ventilation, timely replacement of old batteries, and avoiding overcharge of the battery (3). The main prevention control for thermal runaway will be monitoring of temperature during operation. Battery management systems are used for monitoring and managing the state of the battery and reporting back data to the user. Battery management systems also ensure a controlled environment by making necessary changes to the battery's environment to avoid the possibility of a safety hazard.

Overcharge can result in problems to the battery such as premature aging of the battery through decomposition. Charging regulations that must be considered include the following (1926.441(a) OSHA):

- Battery charging installations shall be located in areas designated for that purpose. (1926.441(b)(1))
- Charging apparatus shall be protected from damage by trucks. (1926.441(b)(2))
- When batteries are being charged, the vent caps shall be kept in place to avoid electrolyte spray. Vent caps shall be maintained in functioning condition. (1926.441(b)(3))

Handling at high operating temperatures requires proper ventilation of the battery's circuit and system. Proper ventilation for the magnesium air battery is necessary to avoid possible damage to the battery, particularly from pressure buildup inside the containment cell. In addition, heat exchangers are needed to take heat from the outlet air, using it to heat the inlet air. Without this heat exchanger system, the entering air may be cold enough to freeze the molten salt electrolyte around the air cathode, causing potential air blockage and failure. A functionality issue among magnesium batteries which must also be noted are parasitic reactions. This can lead to a limitation in the power supply due to the requirement of excess energy in the conversion process of magnesium from an electrolyte to a solid electrode. Potential parasitic reactions which may occur for this system include the following; oxidation of cathode materials leading to oxide scale or dissolution; reduction of nitrogen; reduction of sodium or potassium and their dissolution into the bath - which could create electronic conductivity and reduce current efficiency.

The battery's insulation will be an underlying critical category in its success. With the battery lab-scale demonstration unit currently operating anywhere from 420-620 degrees Celcius we must ensure the insulation is adequate to both retain this heat for proper battery operation and protect the system as a whole against it. In this particular application, the insulation will be directly exposed to molten salt, while also experiencing constant deterioration from flow/motion of the molten salt, produced by whatever transportation system the battery is installed on. Finally cavitation erosion is another possibility within our application of the insulation as bubbles will be present within the design. These factors lead to the problem of heavy degradation and corrosion of the insulating material.

There are already some preexisting solutions that may require only minor tweaks and design changes to meet our application. Insulating fire bricks are classified as refractory products

that are shaped into bricks which typically have a porosity of around 45% as well as an application temperature that is greater than 800 °C (10). Usually, these ceramic refractory materials are used to form a thermal barrier in between a container wall and some high temperature contents. They are also used to hold up under physical stress and to resist erosion as a result of the high temperature content. Finally, insulation fire bricks are used to prevent corrosion and provide thermal insulation.

They are most typically used to form the insulation lining in kilns, reactors, furnaces and any other container that holds and transports hot metal and slag. In addition, refractory materials can be used in other capacities such as hydrogen or ammonia reformers, utility boilers or air heaters (10). Insulation fire bricks are typically created from refractories of aluminum silicate, silicate or lightweight corundum.

Aluminum silicate bricks are the most commonly used type of insulating fire brick. As an insulating material, one of the most important metrics for evaluating the merit of a type of insulating fire brick is the thermal conductivity which is measured in watts per meter Kelvin (W/mK). The qualities of an insulating fire brick are most importantly determined by the porosity, firing temperature and the chemical composition. An insulating fire brick with low density and fine pores will consequently have lower thermal conductivity. On the other hand, the fire brick should also have sufficient density in order to maintain structural integrity under the hot temperatures that it needs to be used in (8).

Insulating fire bricks are classified by a few different standards. The most commonly used are ASTM C115, ISO 2245 and EN 1094-2. These standards all basically classify the firebricks by their density and classification temperature which is based on how much the material shrinks under different temperatures.

For the purpose of the magnesium air battery insulation, fire bricks with higher alumina content are preferred. This is due to alumina's high melting point of 2072 °C, high strength, and low solubility in the molten salt electrolyte. An insulating fire brick with an alumina (Al₂O₃) content of approximately 48% or more is typically considered to be a high alumina firebrick (7). One of the advantages of high alumina fire bricks is the high refractoriness which is the ability for the material to be exposed to high temperatures without experiencing deformation to its structure. On the low end, high alumina bricks will have a refractoriness of around 1750 °C and on the high end, with more alumina content, the refractoriness can be up to around 1900 °C. (7). High alumina firebrick with 70% alumina content costs approximately \$230 for 25 bricks of dimensions 9" x 4.5" x 2.5". (8)

Furthermore, with the addition of higher silica and alkali metal content, the refractoriness under load increases as well with certain types having around 1600 °C as compared to approximately 1430 °C to 1520 °C refractoriness of other fire clay bricks. Lastly, high alumina fire brick tends to have a higher resistance to slag erosion (7).

On the other hand, one disadvantage of high alumina fire bricks is that they have a lower thermal shock resistance as compared to other fire clay bricks. (7). It may also pose issues in integrating the bulky bricks into the current prototype. Another issue is the team doesn't know if

the fire brick, high alumina or not will be able to handle the erosive conditions of the battery. Due to this we will look into more expensive alternatives as well.

Methodology

The project had several primary objectives in the development of the battery, which were meant to explore critical aspects of the design. These objectives can be described as follows. The first objective was to study the rate of corrosion and effectiveness of different types of insulation. The insulation is critical to the operational safety of the battery, so testing different types of insulation materials is good information for future design specifications. In addition, some of the insulation will be exposed to the molten salt, which creates conditions that accelerate corrosion. As a result, the insulation options should also be tested to determine their corrosion rate under an approximation of the battery conditions. Insulation inside of the battery needs to be able to withstand corrosion for a significant length of time, since replacing the inner insulation would require taking the battery apart, which is time-consuming, and prevents further operation.

The second objective was to study the corrosion of the cathode under the internal operating conditions of the battery. There are three main materials that are most optimal for the cathode, which are porous nickel, porous titanium, and porous stainless steel. Specifically, the stainless steel materials of interest are FeCrAl alloys which form alumina scale, possibly with nickel. These materials are generally effective in withstanding extreme heat and corrosive conditions, but the conditions of the battery are fairly unique, so there is very little data on how quickly these materials would corrode. As such, it is necessary to measure the extent of corrosion of the selected cathode samples, in order to determine how often these parts would need to be replaced.

The final objective was to assess the safety of the battery system. The battery is operating at extremely high temperatures, and is responsible for power generation, so determining any risks to surrounding operators and other individuals is critical. Therefore, it is necessary to evaluate what safety risks there are with the battery, and determine adequate solutions to stop or minimize said risks.

Cathode Corrosion

In terms of methodology, the study of the cathode sample corrosion was conducted through a discharge test of the battery. The setup for the discharge tests were conducted as follows. First, the salt mix was prepared in a graphite crucible, with 163.6 g $MgCl_2$, 261.6 g NaCl, and 392.4 KCl measured and mixed into the crucible. Second, the crucible was placed into a box furnace for 3 hours at a temperature of 300 °C, in order to pre-bake it for the battery process. Third, while the prebake was conducted, the cage, anode, cathode, “cold finger”, and ceramic insulation pieces were assembled fully, including the cathode mesh. The final cage construction is shown in Image 1. The first mesh tested was porous titanium, but porous nickel was tested afterwards as well. Critically, the porous titanium has smaller pore sizes than that of the nickel. Fourth, the prebake was completed, and the salt was allowed to cool before being

stored in a plastic container for final setup. Fifth, 50.0 g of NH_4Cl was measured and mixed with the rest of the prebaked salt in the graphite crucible. Sixth, the crucible was secured in the cage, and the cage was lowered into the containment cell and secured with clamps. The cold finger, cathode, and anode were also marked with a sharpie to show their location relative to the crucible. The secured cage and containment cell is shown in Image 1. Seventh, the battery furnace was heated to 250 °C at a 10 °C/min rate, and held at this temperature for two hours. While this was conducted, the wiring for the cage and data collection machine was completed, along with the argon and gas flow connections. Three resistors were also connected to the battery in order to measure the voltage with electrical resistance. Argon was also run through the battery to purge remaining air during the ramping period. Eighth, the furnace temperature was increased to 550 °C at the prior rate. Finally, once the furnace was at 550 °C, the argon flow was shut down, and the air flow was opened for the cathode and cold finger. In addition, the cathode, anode, and cold finger were lowered into the crucible, and the data logger was turned on, in order to collect voltage data from the battery.



Image 1: Final setup of the Magnesium-Air Battery containment cage, including the cathode, anode, cold finger, and crucible.

After this setup, the battery was allowed to discharge for 24 hours, with periodic checkups on its voltage and condition. After this 24 hour period, with all of the voltage data automatically collected, the airflow and furnace were shut down, and the battery was allowed to cool down for subsequent cleanup. Cleanup required the removal of rust from most of the cage and battery components. The remains of the anode and cold finger were recovered, and the end

of the cathode tube was cut off for subsequent mounting and optical examination. The cage after being removed from containment is shown in Image 1. Meanwhile, the mounted titanium and nickel mesh samples are seen in Images 12 and 13. These samples were then examined through surface metrology, which is discussed further in the results.

Insulation

In order to test the insulation material for the battery, the material has to be exposed to the molten salt that is contained within the battery for an extended period of time in order to observe the effects of how the material is broken down. A testing time of 3 hours was deemed sufficient to analyze the reaction of the material and the salt. The material also should not be submerged motionless in the solution because in order to simulate the movement of the battery on a ship, airplane or other vehicle it would be used in, the experiment should continuously move or swirl the material around in the solution throughout the duration of the testing experiment. The motion will accelerate the rate of reactions and ensure that the testing material will be able to stand up to the most strenuous conditions that it may face during its use in practical applications without resulting in a leak or any other catastrophic failure. The subsequent testing examined these areas as follows.

The first experiment with the insulation was conducted as follows. Two types of firebrick insulation were tested, a standard refractory firebrick, and a 70 % high alumina firebrick. Two pieces of these bricks were chiseled off the main brick for the purpose of further testing. First, the refractory and high alumina bricks were put into separate graphite crucibles, which were respectively noted as Crucible 1 and Crucible 2. Second, 41.2 g $MgCl_2$, 66.1 g $NaCl$, and 98.0 g of KCl were weighed and mixed into Crucible 1, along with the standard refractory brick sample. Third, 41.4 g $MgCl_2$, 66.3 g $NaCl$, and 98.2 g of KCl were weighed and mixed into Crucible 2, along with the high alumina brick sample. Both samples were submerged halfway in the salt, and marked in order to show where they were submerged, for future examination. These weights were a replication of the weight ratios used in the standard battery experiments prior to the project. NH_4Cl was not included in the crucibles, since its toxicity would be dangerous in an uncontained furnace, and would make the cleanup process more difficult. Fourth, both crucibles were placed in a foundry furnace, with a cover of scrap sand casting molds to cover the crucible top. These crucibles were also placed in larger graphite crucibles, as a means of secondary containment. This was to prevent molten salt from moving out of the crucible during the test, especially in the event of a crack in the primary crucible. Fifth, the furnace was closed and set to an operating temperature of 600 °C. Sixth, both crucibles were kept in the furnace at this operating temperature for 18 hours, allowing the salt to fully melt with the brick inside the crucible. After 18 hours, the furnace was shut down and allowed to cool for another 12 hours. Finally, the crucibles were taken out of the furnace after cooling, and the brick samples were removed from the crucibles. The crucibles and samples were then cleaned and stored for future preparation.

The second test was conducted very similarly to the first test, with a few differences. The crucible numbers for the respective refractory and high alumina bricks were kept the same, as crucibles 1 and 2. The secondary containment was also the same, along with the primary containment and scrap casting sand lid. For the salt mixture, 65.4 g MgCl₂, 104.7 g NaCl, and 150.1 g of KCl was weighed and mixed into Crucible 1. Meanwhile, Crucible 2 contained 65.3 g MgCl₂, 104.6 g NaCl, and 150.0 g of KCl. The experiment was conducted at a temperature of 600 °C, but the length of the experiment was increased to 68.5 hours. Once all of the experimental brick samples were recovered, they were stored for potential microscope preparation. The first step in this process was cutting a 0.75 by 0.75 inch square with a thickness of 0.5 inches. This was done for all of the experimental samples, specifically the section of the brick submerged in the salt. The unsubmerged brick sections from experiment 2 were also recovered in the same way, along with unused samples of both brick types for comparison. In total, there were eight samples cut for the purpose of polishing. Next, these samples were polished in order to keep their surface smooth. Without a smooth surface, the microscope would be unable to focus on the sample and its specific features.

Once the polishing was completed, a total of eight samples were examined under the microscope. This included two samples of untested brick as a point of comparison. Critically, in experiment 2, there were samples taken from the submerged and unsubmerged parts of the brick, since there were interesting features on the unsubmerged part of both brick types. The samples were also studied through a surface metrology microscope, and the results of these examinations are discussed further in the results section.

Battery Safety

It is also important to note that the magnesium air battery has been designed to have greater energy storage potential at very high operating temperatures. When assessing the safety of the battery system there are many safety hazards that must be accounted for. For this, the process of failure modes and effects analysis (FMEA) was implemented. FMEA involves the process of reviewing all components of the system to identify potential failure modes and their cause and effects through effects analysis. Detection, occurrence, and severity are used in calculating the risk priority numbers for individual failure modes (6). This is given by the following equation:

$$\text{RPN} = \text{severity} \times \text{occurrence} \times \text{detection}$$

If safety problems arise it is recommended that attention be focused on failures with the highest RPN scores (6). Typically, these RPN calculations for each situation, along with subsequent countermeasures, are displayed in an FMEA table. The FMEA was conducted on the battery in this manner, by studying multiple types of failures, their dangers, and what can be done to mitigate or outright prevent them. From the RPN calculations, the five highest-priority safety concerns were identified. All FMEA results were also compiled into the FMEA table. The overall results of the insulation, cathode, and FMEA methods can be seen in the results section.

Results

Insulation

After the tests were conducted regarding the cathode and insulation samples, as described in the methodology, there were several trends in the damage patterns in these samples, which are discussed as follows. The first materials under examination are the insulation samples, specifically the refractory brick and high-alumina brick. There were two prepared material samples from the first insulation test, with one sample of each material type. In addition, there were four prepared material samples from the second test, with two of each material type. Finally, there were two samples of untested brick as controls, one of each material type. The first testing method was surface metrology, which used a gel press and camera to map the surface of the samples, as well as their significant topographical features. Each surface metrology measurement covered an area approximately 1mm x 1mm. To begin, the surface metrology images of the high alumina and refractory samples for the first experiment are seen in Images 2 and 3, respectively. Before explaining the results, there are two critical terms that need to be mentioned, kurtosis and max peak. Kurtosis is a measure of the relative sharpness of the features of the surface. A higher kurtosis magnitude usually indicates more significant surface damage. Meanwhile, max pit is the maximum depth of the surface damage in the sample. In the samples from experiment 1, the high alumina brick sample had a kurtosis and max pit of 2.49 and 430, respectively. Meanwhile, the refractory brick sample had a kurtosis and max peak of 2.85 and 151, respectively. Interestingly, when examining the sample images, the significantly higher max pit of the high alumina sample was due to a deep gash in the sample, which was the result of damage during the polishing process. Still, even given this error, the high alumina had a lower kurtosis than the refractory brick, which suggests that the refractory sample had more jagged damage than that of the high alumina. This suggests that the refractory brick suffered a larger overall loss in material than the high alumina brick, which is also reinforced by the images since the high alumina sample is relatively undamaged aside from the polishing mistake. Meanwhile, the entire surface of the refractory sample had been damaged.

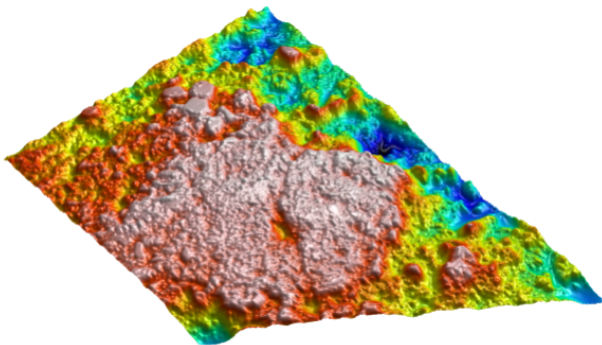


Image 2: Surface metrology height map image of the high-alumina brick sample from the first insulation test. This sample was partially damaged during the polishing process. This sample had a kurtosis and max pit of 2.49 and 430, respectively.

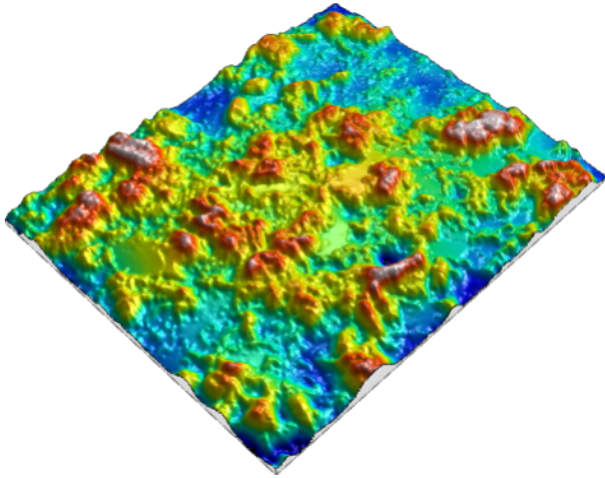


Image 3: Surface metrology height map image of the refractory brick sample from the first insulation test. This sample had a kurtosis and max peak of 2.85 and 152, respectively.

The second test had results that reinforced this conclusion. In the second test, two samples were taken of each brick, one from the lower part, which was exposed to salt, and one from the upper part, which was not. To begin, the images of the lower high alumina and refractory samples can be seen in Images 4 and 5, respectively. The kurtosis and max pit values of the high alumina sample are 4.80 and 1770, respectively. Meanwhile, the respective kurtosis and max pit values of the refractory sample are 10.6 and 326. As seen in this data and the associated images, the refractory brick had significantly deeper surface damage than the high alumina brick.

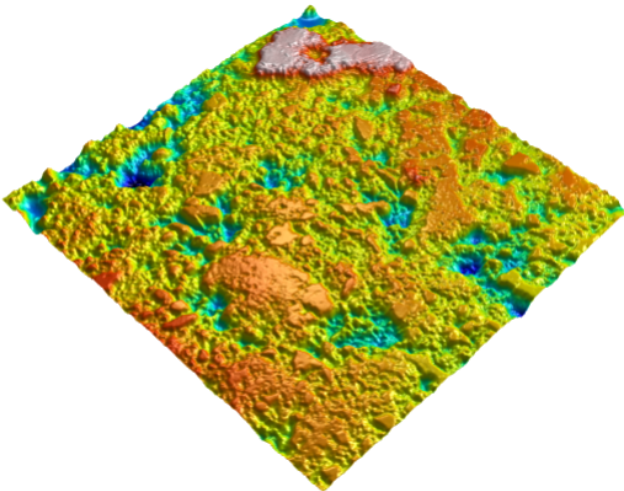


Image 4: Surface metrology height map image of the lower high-alumina brick sample from the second insulation test. This sample had a kurtosis and max pit of 4.80 and 177, respectively.

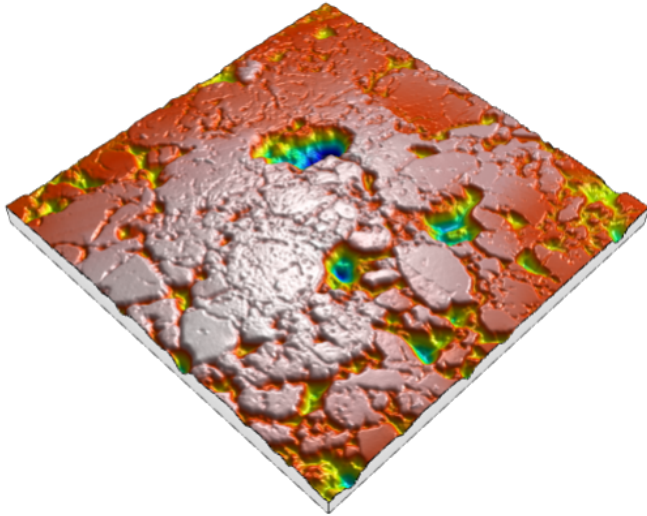


Image 5: Surface metrology height map image of the lower refractory brick sample from the second insulation test. This sample had a kurtosis and max pit of 10.6 and 326, respectively.

The upper images of the high alumina and refractory samples can be seen in Images 6 and 7, respectively. From these images, the respective kurtosis and max pit values of the high alumina sample are 7.85 and 248. Meanwhile, the refractory sample had respective kurtosis and max pit values of 5.18 and 250. Interestingly, the refractory sample had a slightly lower kurtosis than that of the high alumina, likely because these samples were not exposed to the molten salt. However, even discounting the salt exposure, the refractory sample still had a slightly higher max peak, which suggests that the heat alone can cause deep defects in the refractory brick.

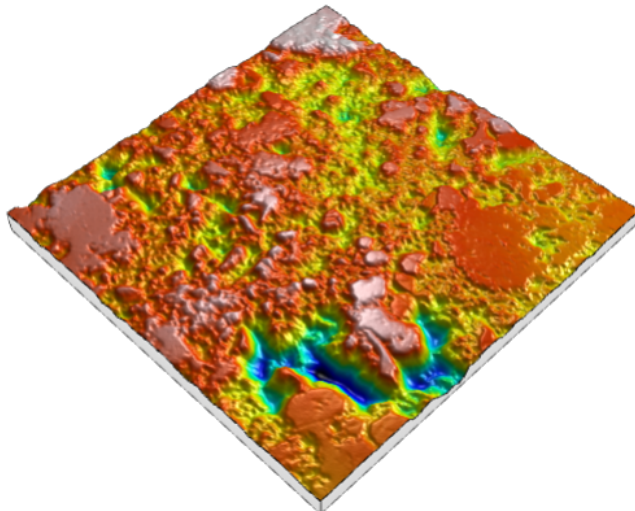


Image 6: Surface metrology height map image of the upper high-alumina brick sample from the second insulation test. This sample had a kurtosis and max pit of 7.85 and 249, respectively.

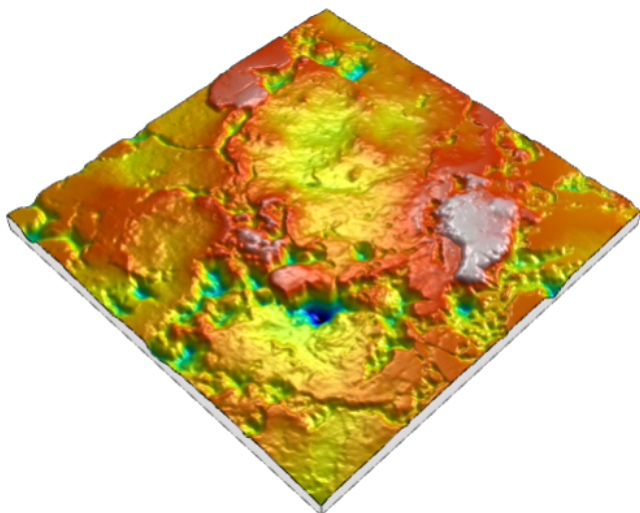


Image 7: Surface metrology height map image of the upper refractory brick sample from the second insulation test. This sample had a kurtosis and max pit of 5.18 and 250, respectively.

The final samples under study were of both brick types, but were not exposed to any heat or molten salt. These samples and their topography are seen in Images 8 and 9. The undamaged high alumina sample had respective kurtosis and max pit values of 33.5 and 147. Meanwhile, the undamaged refractory sample had respective kurtosis and max pit values of 30.0 and 284. These values are similar to each other, but the refractory has a deeper max pit than the high alumina. This weakness allows salt to flow deeper into the refractory brick, causing more internal damage than the high alumina brick. As such, the high alumina brick is likely a better choice for internal battery insulation.

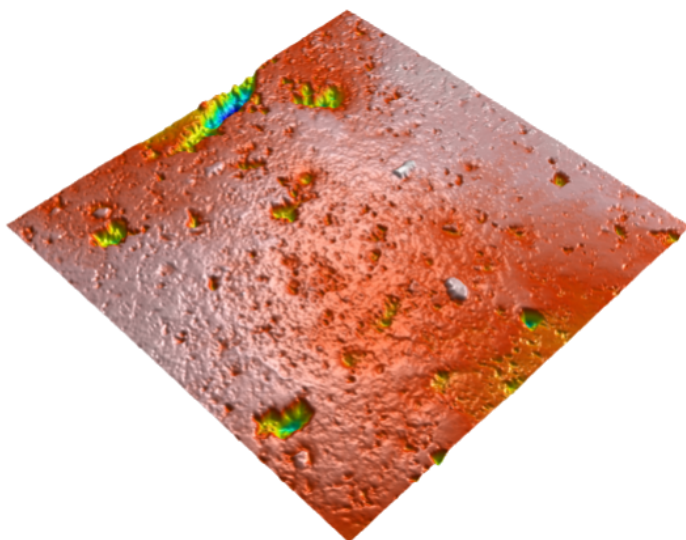


Image 8: Surface metrology height map image of the undamaged high-alumina brick sample. This sample had a kurtosis and max pit of 33.5 and 147, respectively.

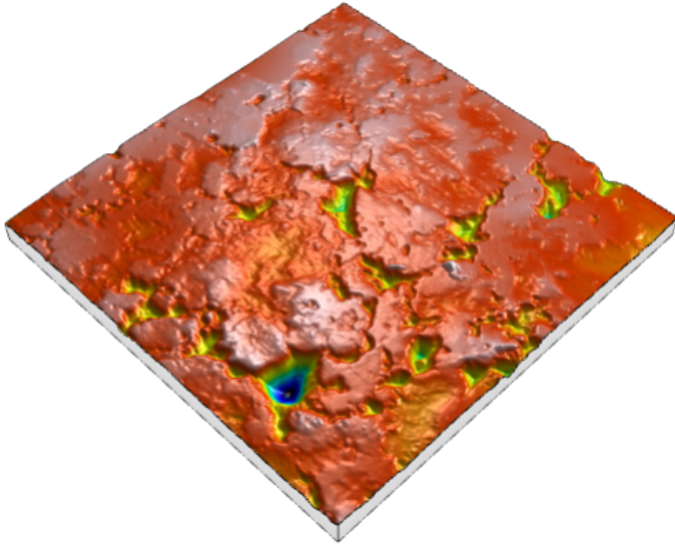


Image 9: Surface metrology height map image of the undamaged refractory brick sample. This sample had a kurtosis and max pit of 30.0 and 284, respectively.

Cathode

The examination of both cathode samples was primarily conducted through surface metrology examination and mapping. The results of this testing are as follows. To begin, it is important to note that measurements of kurtosis and max pit were not nearly as indicative of damage in this sample as they were with the insulation. It was particularly difficult to obtain exposed surface area with the cathode. In addition, since the rest of the cathode aside from the mesh was mounted in smooth resin, measuring the cathode area that was not exposed was not feasible. Fortunately, the topographical images from the surface metrology testing showed insight into the effectiveness of each mesh.

The height map of the nickel cathode mesh sample from the first experiment can be seen in Image 10. As seen in this height map, the pores of the cathode mesh are still clearly visible, even after exposure to the battery. This can also be seen in the cross-section of the cathode, seen in Image 12. In addition to the mesh and its pores being clearly visible, there is no salt content past the mesh, suggesting that the salt was unable to breach the mesh during the experiment. As for the titanium mesh sample from the second experiment, the results are more interesting. As seen in the height map in Image 11, the titanium mesh has fewer visible pores, but there are still some porous areas in the mesh. In addition, as seen in the cross-section in Image 13, there are still porous areas of the mesh, and more critically, there does not seem to be any salt past the mesh. This suggests that the mesh was able to stop salt flow from reaching the cathode while keeping its porosity.

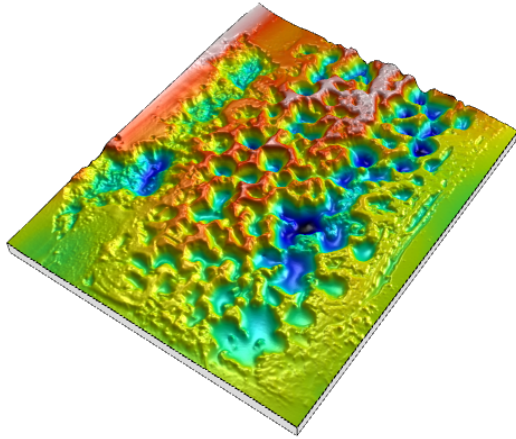


Image 10: Surface metrology height map of the nickel cathode sample from the first cathode test.

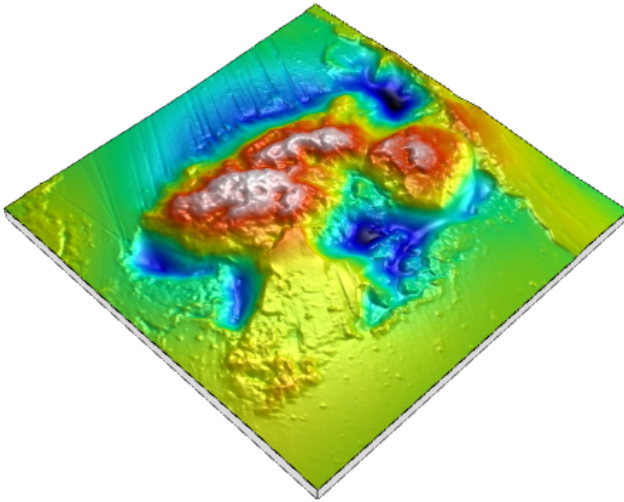


Image 11: Surface metrology height map of the titanium cathode sample from the second cathode test.

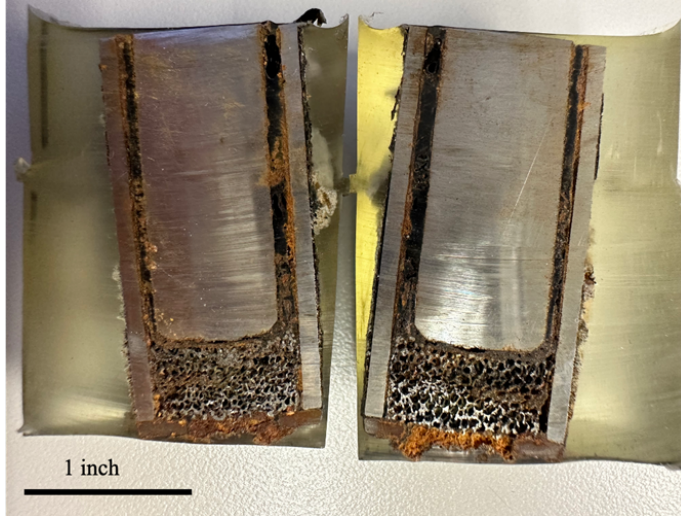


Image 12: Porous nickel cathode mesh sample from the first cathode test. The cathode was cut in half to reveal its cross section, as seen in the image.



Image 13: Porous titanium cathode mesh sample from the second cathode test. The cathode was cut in half to reveal its cross section, as seen in the image.

FMEA

The FMEA results were conducted through the FMEA table, which is shown in full in Table 1 (in the Appendix). The relative meanings of each number value for severity, occurrence, and detection can also be found in Table 2 (Appendix). The top highest-risk priorities were found to be as follows:

1. Plating in battery
2. Dendrite formation
3. Stripping in battery
4. Insufficient air drying

5. External electrical shortages

Plating within the battery may result in reduced battery capacity and had the highest calculated RPN of 392. Recommended actions to avoid this include the implementation of electrical current sensors, preventing overcharge or charge at low temperatures, and regular inspection after shutdown which is also recommended to avoid plating in the battery. Second on our team's risk priority list (RPN=280) was dendrite formation within the battery. Dendrite formation can result in a battery shortage or failure. This could also result in a possible fire or explosion as a result. Avoiding irregular charging and implementing an automatic shutdown connection should be used for monitoring the charging of the battery. Third in risk priority (RPN=224) was stripping in the battery which can result in internal oxidation. This could be prevented by introducing an additive chemical for reaction prevention. NH_4Cl was already added to prevent this, but research into other additive chemicals should be further explored. The fourth highest RPN was insufficient air drying to the battery (RPN=224). Insufficient air drying is caused by blocked air circulation and may result in accelerated corrosion. This can be avoided by regular air circulation inspections and the implementation of airflow sensors in potential risk areas. Lastly on the ranking of the five highest risks in battery operation, was external electrical shortages. This is because an interaction between the electrical shortage and the battery or surrounding systems could result in a fire or potential injury to operators. As such, regular component inspections on the system should be done to avoid this, and the surrounding electrical systems should be regularly monitored.

Conclusion

The experimental results of the insulation, cathode, and FMEA testing had several specific trends, which are the basis for the following suggestions regarding each objective. With regards to the insulation, the recommendation is to use high alumina material as opposed to standard refractory firebrick material. The reason for this recommendation is due to the higher refractoriness, higher resistance to heat and corrosion, and higher slag resistance of refractory material with higher alumina content. Our experimental results supported these research findings by a noticeable and measurable difference between the damage done to the different types of refractory material when placed in a furnace with the battery salts to attempt to simulate battery operation conditions. These measurements included parameters that characterize surface roughness and porosity, analyzed with the aid of a GelSight surface metrology microscope as well as visually recorded observations done before and after exposure to the battery conditions. Some research also indicates that higher silica and alkali metal content in refractory materials also leads to higher corrosion resistance, so further research into the use of these materials is also recommended.

In addition, our project evaluated the use of nickel and titanium materials in the cathode of the battery. Both materials were used as a cathode during a typical battery testing protocol. The recovered materials were evaluated under the GelSight surface metrology microscope to

analyze the aftereffects of the battery operation on each cathode material. The results indicated that both cathode samples were effective in allowing airflow through the cathode while blocking salt from leaking into the cathode. As such, the results suggest that either porous nickel or porous titanium is sufficient for the continued operation of the battery. However, the testing for these cathode materials was very limited in terms of time. These samples were only tested for 24 hours, but a pilot-scale battery would be running for a period of several weeks, at least. Therefore, additional testing for longer periods of time is necessary to gain a full picture of the capabilities of these materials. In addition, it may be wise to test other materials, such as porous stainless steel and porous tungsten, to determine their effectiveness for the battery design. Kanthal is a particular stainless steel alloy that may be functional for the cathode mesh, due to its heat and corrosion resistance (9). Finally, there are forms of anticorrosive coating, such as titanium nitride (TiN), which are used commonly in multiple different industries. Testing these coatings under the battery's operating conditions may be wise for the future development of the battery system.

Finally, an FMEA analysis highlighted the most pertinent safety issues to be addressed during the further development of the magnesium air battery technology. According to our research, plating in battery, dendrite formation, stripping in battery, insufficient air drying, and external electrical shortages were the most crucial areas of focus with the most pertinent issue listed first. Electrical current sensors were the first recommendation for abating the effect of battery plating. Attention should be paid to avoid overcharging and charging at high temperatures as well as thorough and regular evaluation of the battery after operation are other recommendations to best manage the issues of battery plating and dendrite formation. In addition, avoiding stripping within the battery through reaction prevention, allowing sufficient air drying to the battery, and monitoring external electrical components to avoid possible fire and safety risks should also be accounted for. Overall, the objectives of this project acted as solid groundwork for future research on the effectiveness of different materials for the critical components of the battery. This research, and research in the future, may be helpful in progressing the battery to a pilot-scale device, and potentially beyond that point.

Works Cited

1. Al Mutaz, I. S.; Wagialia, K. M. Production of Magnesium from Desalination Brines. *Resources, Conservation and Recycling* 1990, 3 (4), 231–239. [https://doi.org/10.1016/0921-3449\(90\)90020-5](https://doi.org/10.1016/0921-3449(90)90020-5).
2. Chen, L., Lan, H., Huang, C., Yang, B., Du, L., & Zhang, W. (2017). Hot corrosion behavior of porous nickel-based alloys containing molybdenum in the presence of NaCl at 750 °C. *Engineering Failure Analysis*, 79, 245–252. <https://doi.org/10.1016/j.engfailanal.2017.05.009>.

3. Dragonfly Energy. "What Is Thermal Runaway in Batteries?" *Dragonfly Energy*, 21 July 2022, <https://dragonflyenergy.com/thermal-runaway/>.
4. Eymen. "Fuses: The Basics." *Battery Design*, 17 Jan. 2022, <https://www.batterydesign.net/fuses-the-basics/>.
5. Ehrenberger, S.; Friedrich, H. E. Life-Cycle Assessment of the Recycling of Magnesium Vehicle Components. *JOM* 2013, 65 (10), 1303–1309. <https://doi.org/10.1007/s11837-013-0703-3>.
6. Forrest, George. "FMEA (Failure Mode and Effects Analysis) Quick Guide." *ISixSigma*, 26 Mar. 2020, <https://www.isixsigma.com/tools-templates/fmea/fmea-quick-guide/>.
7. *High alumina fire bricks - RS refractory bricks manufacturer*. Quality RS Refractory Fire Bricks For Sale. (2022, September 2). Retrieved October 13, 2022, from <https://rsrefractoryfirebrick.com/high-alumina-fire-bricks/>
8. *High alumina hard firebrick 3245°F*. *CeraMaterials*. (2022, March 8). Retrieved October 13, 2022, from <https://www.ceramaterials.com/product/high-alumina-hard-brick/>
9. Sarikka, Teemu; Iloa, Risto; Pohja, Rami; Hänninen, Hannu. Corrosion resistance of Kanthal A-1 and Fe-12Cr-2Si alloy coatings in Cl-containing environment. *Aalto University School of Engineering, Department of Engineering Design and Production. VTT Technical Research Centre of Finland*. June 2013.
10. Says:, S. R., & Says:, R. (2018, November 21). *Insulating fire bricks - production, properties, classification, literature*. insulatioNet.com. Retrieved October 13, 2022, from <http://insulationet.com/en/insulating-fire-bricks/#:~:text=Insulating%20fire%20bricks%20are%20aluminum.classification%20of%20the%20refractory%20bricks>.
11. Seah, K. H. W., Thampuran, R., Chen, X., & Teoh, S. H. (1995). A comparison between the corrosion behaviour of sintered and unsintered porous titanium. *Corrosion Science*, 37(9), 1333–1340. [https://doi.org/10.1016/0010-938x\(95\)00033-g](https://doi.org/10.1016/0010-938x(95)00033-g).
12. "United States Department of Labor." 1926.441 - *Batteries and Battery Charging*. | *Occupational Safety and Health Administration*, <https://www.osha.gov/laws-regs/regulations/standardnumber/1926/1926.441>.

Appendix of Tables

Process Actions (Function)	Potential Problems (Failure Mode)	Outcomes of Problems (Effects)	Severity	Causes of Problems (Failure Cause)	Occurrence	Current Process Controls (What Fails the Problem Today?)	Detection	Priority #	Recommended Actions That Address Problem	Responsible Party and Target Completion Date	Actions Taken	Severity	Occurrence	Detection	RPN
Purge O2 with Argon	O2 doesn't decrease	Battery failure	8	Forget to connect Argon	1	written procedure, ext O2 sensor	2	16	Sensors that will alarm when there is no Argon						
Purge O2 with Argon	O2 doesn't decrease	Battery failure	8	Forget to turn on Argon regulator	2	written procedure, ext O2 sensor	2	32	Sensors that will alarm when there is no Argon						
Purge O2 with Argon	O2 doesn't decrease	Battery failure	8	Argon supply is exhausted	2	written procedure, ext O2 sensor	2	32	Sensors that will alarm when there is no Argon						
Purge O2 with Argon	O2 doesn't decrease	Battery failure	8	System outlet connection is blocked	1	written procedure, ext O2 sensor	2	16	Different material use (Stainless Steel)						
Purge O2 with Argon	Pressure builds up in system	Apparatus compromised	10	System outlet connection is blocked	2	no pressure relief built in, except for seals	3	60	Pressure relief valves and maybe rupture disks						
Purge O2 with Argon	O2 decreases very slowly	Battery failure	8	Breach in Argon connection	1	Plastic tubing, no fail-safe systems.	3	24	System shutdown from sensor, replacement tubing, tubes made of stronger type of plastic or other material						
Battery Operation	Thermal runaway	Battery failure or explosion	10	Overproduction of energy	2	Proper storage temperatures for battery	2	40	Monitoring temperature during operation, sensors connected to PID control software and a fail system shutdown, imply coolant system						
Battery Operation	Dendrite formation	Battery shorage, battery failure, possible fire or explosion	10	Irregular charging	4	Monitor charging	7	280	Current monitor systems, Automatic shutdown connection for abnormal current, Regular inspection after shutdown.						
Battery Operation	Stripping in Battery	Oxidation of surface atoms on battery	8	Release of cations onto electrolyte	4	N/A	7	224	Introduce additive chemical for reaction prevention						
Battery Operation	Containment Failure or Breach	Battery failure, possible fire, possible explosion	10	Corrosion of the containment cell, internal runaway reactions, internal pressure buildup	2	Monitor containment cell, temperature and pressure sensors	2	40	Fire protection and secondary containment. Secondary containment should have gravel in larger trenches around the battery						
Battery Operation	Temperature becomes too high	Melting of magnesium	7	High Temperatures	4	Temperature sensors, relief valves, fire protection	7	196	Have proper cooling systems in place as well as shutdown warnings to prevent battery damage						
Battery Operation	Pfeling in Battery	Reduces battery capacity	7	Metal deposited on surface of anode	8	Electrical current sensors	7	392	Prevent overcharging, avoid charge/discharge at low temperatures, regular inspection after shutdown.						
Transport	Lateral instability	Damaged components	8	Improper transportation/ loading procedure / Faulty external equipment	3	N/A	6	144	Ensure securing procedures are in place and strictly followed						
Loading	Dropped container	Damaged components	8	Improper transportation/ loading procedure / Faulty external equipment	3	N/A	4	96	Ensure proper loading/transportation procedures are strictly followed						
Loading, Transport	Container puncture	Damaged components	8	Improper transportation/ loading procedure / Faulty external equipment	3	N/A	4	96	Ensure proper loading/transportation procedures are strictly followed						
Battery Operation	Insulation failure	Damaged components	8	Containment / Insulation erosion	4	N/A	4	128	Ensure routine maintenance and checks are done on insulation and containment						
Loading	Excessive top loading	Damaged components	8	Improper transportation / loading procedure / Faulty external equipment	3	N/A	4	96	Ensure proper loading procedures are in place and strictly followed						
Discharge	Insufficient air drying	Faster corrosion	7	Blocked air circulation	4	Regular air circulation inspections	8	224	Air flow sensors at potential risk areas						
Transport	Poor securing in transit	Damaged components	8	Improper transportation / loading procedure / Faulty external equipment	3	N/A	4	96	Ensure securing procedures are in place and strictly followed						
Discharge	Salt fume/heat escape/dispersion	Health hazard - LD50	6	Loose components / Broken seals	4	Regular component inspections	2	48	Cyclone separators, fans or other HVAC						
Discharge	External electrical short	Safety/Fire Risk	10	Exposed wiring / Bad grounding / Improper electrical safety	3	Regular component inspections	7	210	Follow wiring safety / Inspection protocols						
Discharge	Magnetic field interaction	Health Risk	10	Electronic Interactions	1	Regular component inspections	7	70	Avoid interactions						

Table 1: This is the completed FMEA analysis table for the magnesium-air battery. This table includes a detailed analysis of the severity, occurrence, detection, and RPN values of each identified safety risk, along with additional precautions.

Severity Rating Scale			Occurrence Rating Scale			Detection Rating Scale		
Rating	Description	Definition (Severity of Effect)	Rating	Description	Potential Failure Rate	Rating	Description	Definition
10	Dangerously high	Failure could injure the customer or an employee.	10	Very High: Failure is almost inevitable.	More than one occurrence per day or a probability of more than three occurrences in 10 events ($C_{pk} < 0.33$).	10	Absolute Uncertainty	The product is not inspected or the defect caused by failure is not detectable.
9	Extremely high	Failure would create noncompliance with federal regulations.	9	High: Failures occur almost as often as not.	One occurrence every three to four days or a probability of three occurrences in 10 events ($C_{pk} \approx 0.33$).	9	Very Remote	Product is sampled, inspected, and released based on Acceptable Quality Level (AQL) sampling plans.
8	Very high	Failure renders the unit inoperable or unfit for use.	8	High: Repeated failures.	One occurrence per week or a probability of 3 occurrences in 100 events ($C_{pk} \approx 0.67$).	8	Remote	Product is accepted based on no defectives in a sample.
7	High	Failure causes a high degree of customer dissatisfaction.	7	High: Failures occur often.	One occurrence every month or one occurrence in 100 events ($C_{pk} \approx 0.83$).	7	Very Low	Product is 100% manually inspected in the process.
6	Moderate	Failure results in a subsystem or partial malfunction of the product.	6	Moderately High: Frequent failures.	One occurrence every three months or three occurrences in 1,000 events ($C_{pk} \approx 1.00$).	6	Low	Product is 100% manually inspected using go-no-go or other mistake-proofing gages.
5	Low	Failure creates enough of a performance loss to cause the customer to complain.	5	Moderate: Occasional failures.	One occurrence every six months to one year or five occurrences in 10,000 events ($C_{pk} \approx 1.17$).	5	Moderate	Some Statistical Process Control (SPC) is used in process and product is final inspected off-line.
4	Very Low	Failure can be overcome with modifications to the customer's process or product, but there is minor performance loss.	4	Moderately Low: Infrequent failures.	One occurrence per year or six occurrences in 100,000 events ($C_{pk} \approx 1.33$).	4	Moderately High	SPC is used and there is immediate reaction to out-of-control conditions.
3	Minor	Failure would create a minor nuisance to the customer, but the customer can overcome it without performance loss.	3	Low: Relatively few failures.	One occurrence every one to three years or six occurrences in ten million events ($C_{pk} \approx 1.67$).	3	High	An effective SPC program is in place with process capabilities (C_{pk}) greater than 1.33.
2	Very Minor	Failure may not be readily apparent to the customer, but would have minor effects on the customer's process or product.	2	Low: Failures are few and far between.	One occurrence every three to five years or 2 occurrences in one billion events ($C_{pk} \approx 2.00$).	2	Very High	All product is 100% automatically inspected.
1	None	Failure would not be noticeable to the customer and would not affect the customer's process or product.	1	Remote: Failure is unlikely.	One occurrence greater than five years or less than two occurrences in one billion events ($C_{pk} > 2.00$).	1	Almost Certain	The defect is obvious or there is 100% automatic inspection with regular calibration and preventive maintenance of the inspection equipment.

Table 2: This table includes the relative meanings and descriptions of each numerical value for the severity, occurrence, and detection values in the FMEA analysis table (Table 1).